1 OF 1
ADA
040225
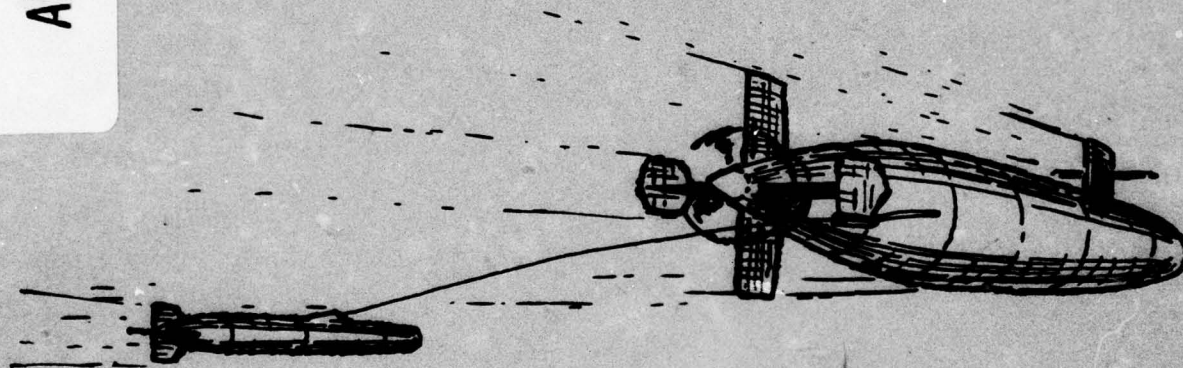
END
DATE
FILMED
6-77

CONTROLLED TOWED ARRAY SURVEILLANCE SYSTEM
(CTASS)

ARRAY STATIC TEST AND SIMULATION

See Form
1473

GENERAL DYNAMICS Corp.
Electric Boat Division

CONTROLLED TOWED ARRAY SURVEILLANCE SYSTEM (CTASS)

Array Static Test and Simulation

by

A. J. Izzo

M. H. Ueberschaer

Contract N00039-76-C-0169

GENERAL DYNAMICS CORPORATION
Electric Boat Division
Groton, Connecticut

Reviewed by: _C. E. Aldrich_
C. E. Aldrich
Manager of Advanced
Systems Engineering

Approved by: _R. A. Abate_
R. A. Abate
Chief Engineer
Advanced Engineering

CTASS-77-01
January 1977

CONTENTS

SUMMARY

The intended purpose of this investigation was to perform a thorough evaluation of the CTASS (Controlled Towed Array Sonar System) concept. This evaluation was to be made under expected typical operation conditions with respect to several performance criteria: detection, resolution, and resistance to acoustic interference. Because of mathematical complexities in the analysis of multiplicative processing systems, the evaluation was to be made largely by simulation. The project consisted of several stages:

1. Collection of sea noise data.
2. Mathematical modeling of CTASS operating on simulated signal and measured noise data.
3. Filtering and digitizing of recorded sea noise.
4. Numerical CTASS performance evaluation.

The first three stages were fully completed. In the fourth stage, numerical CTASS evaluation, the first performance criterion to be evaluated was detection, as measured by the performance index of the output signal-to-noise ratio $(\frac{S}{N})_o$. (For long integration times, detection probability is a function of $(S/N)_o$.) Earlier analysis (which had been possible only to a limited extent) had indicated that there was some reason to believe that $(\frac{S}{N})_o$ might not show any improvement (indeed, might show a decline) as the size of the array increased. It was decided to cease further CTASS evaluation with respect to the other criteria if signal detectability was found not to increase with array size.

Numerical CTASS evaluation showed a definite (and discouraging) decrease in $(\frac{S}{N})_o$ as the array size increased. This was found to be true even at high input signal-to-noise ratios. This prompted a further analysis using noise-free conditions with an idealized sinusoidal input signal, but assuming realistic integration times. This analysis showed a definite decrease in $(\frac{S}{N})_o$ as the array size is increased, resulting in the conclusion that CTASS in its presently conceived configuration is not a promising array processing system. All further evaluation work was therefore halted. Possibly some other configuration using gradient and omnidirectional hydrophones would result in better detection performance. A modification of the present simulation model could be used in that evaluation.

INTRODUCTION

Controlled Towed Array Surveillance System (CTASS) refers to a proposed passive, Towed, Acoustic Surveillance System that would employ a multiplicative array of gradient hydrophones, as compared with the conventional linear summed array of omnihydrophones. CTASS would employ two arrays of nine electrodynamic gradient hydrophones and one omnihydrophone. The two arrays would form an orthogonal set housed in a small controllable hydrodynamic body about 10 inches in diameter and 9 feet long (figure 1). Array gain would be obtained by uniquely processing the output of these hydrophones.

1. PRESSURE TRANSDUCER
2. HEADING SENSOR
3. PITCH AND ROLL SENSOR
4. HYDROPHONE ELECTRONICS
5. COMPENSATION DIAPHRAGM
6. HYDROPHONE ARRAY
7. PLANE CONTROL ELECTRONICS
8. PLANE SERVOS
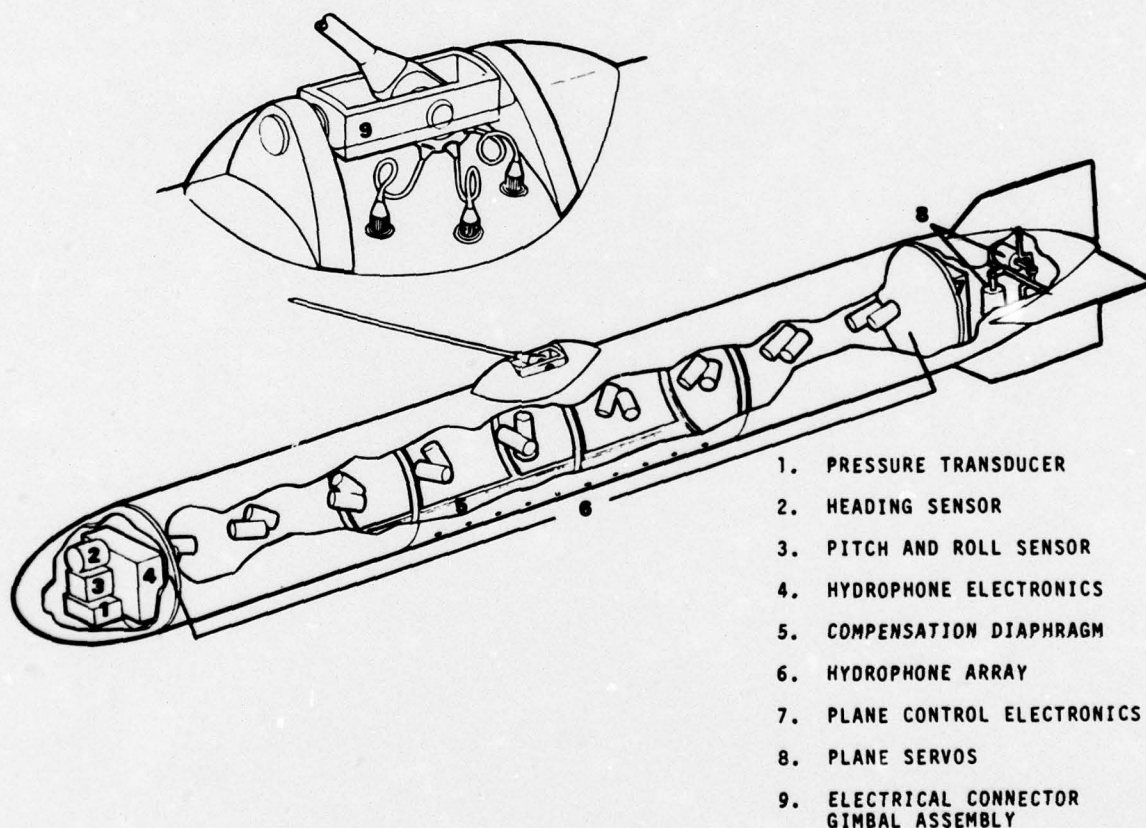9. ELECTRICAL CONNECTOR
   GIMBAL ASSEMBLY

Figure 1. CTASS Towed Vehicle

2

The signal processing would be multiplicative and enhanced by the inter-relationship of the placement and directivity of each hydrophone. Because of the acoustic characteristics of each hydrophone, and the type of signal processing used, the system theoretically would achieve a three-dimensional (pencil-shaped) beam pattern that would be invariant over the frequency range of 10 Hz to 10 kHz.

Each CTASS array would consist of an omnidirectional hydrophone and $2q + 1$ gradient (or dipole) hydrophones. The omnielement and one dipole would be combined to form a cardioid beam pattern. The remaining $2q$ dipoles would be canted relative to the cardioid by progressively larger angles (η), the first pair or section at $\pm \eta^{\circ}$. the second section at $\pm 2\eta^{\circ}$, etc. The array output would be obtained by forming the product of the cardioid output and the outputs of all $2q + 1$ dipoles (i.e., the output would be a product of $2q + 2$ factors). The element outputs would be filtered with narrow band filters, and the product would be low pass filtered, figure 2. Features such as simultaneous processing of multiple frequency channels, simultaneous beamforming, and pencil beams would be available.

The formation of the beam may be described briefly as follows: The first dipole would have nulls at $\pm 90^{\circ}$ from the beam axis. The next pair would have nulls at $\pm 90^{\circ} + \eta^{\circ}$ and $\pm 90^{\circ} - \eta^{\circ}$. The product of these three would have nulls at $90^{\circ} - \eta^{\circ}$, 90°, $90^{\circ} + \eta^{\circ}$, $-90^{\circ} - \eta^{\circ}$, -90°, and $-90^{\circ} + \eta^{\circ}$. The next pair of dipoles would have nulls at $\pm 90^{\circ} + 2\eta^{\circ}$, and inclusion of these in the product would produce a pattern with 5 nulls on each side at spacing η° apart. Continuing in this manner, one would obtain a pattern with $2q + 1$ nulls on each side with quite low sidelobes between the nulls. The pattern thus far would be symmetric fore and aft. The cardioid pattern would have a single null at 180°. Multiplication of the product of the $2q + 1$ dipole outputs by the cardioid output theoretically would destroy the back lobe, and produce a pattern with a single main lobe and $4q + 3$ nulls.
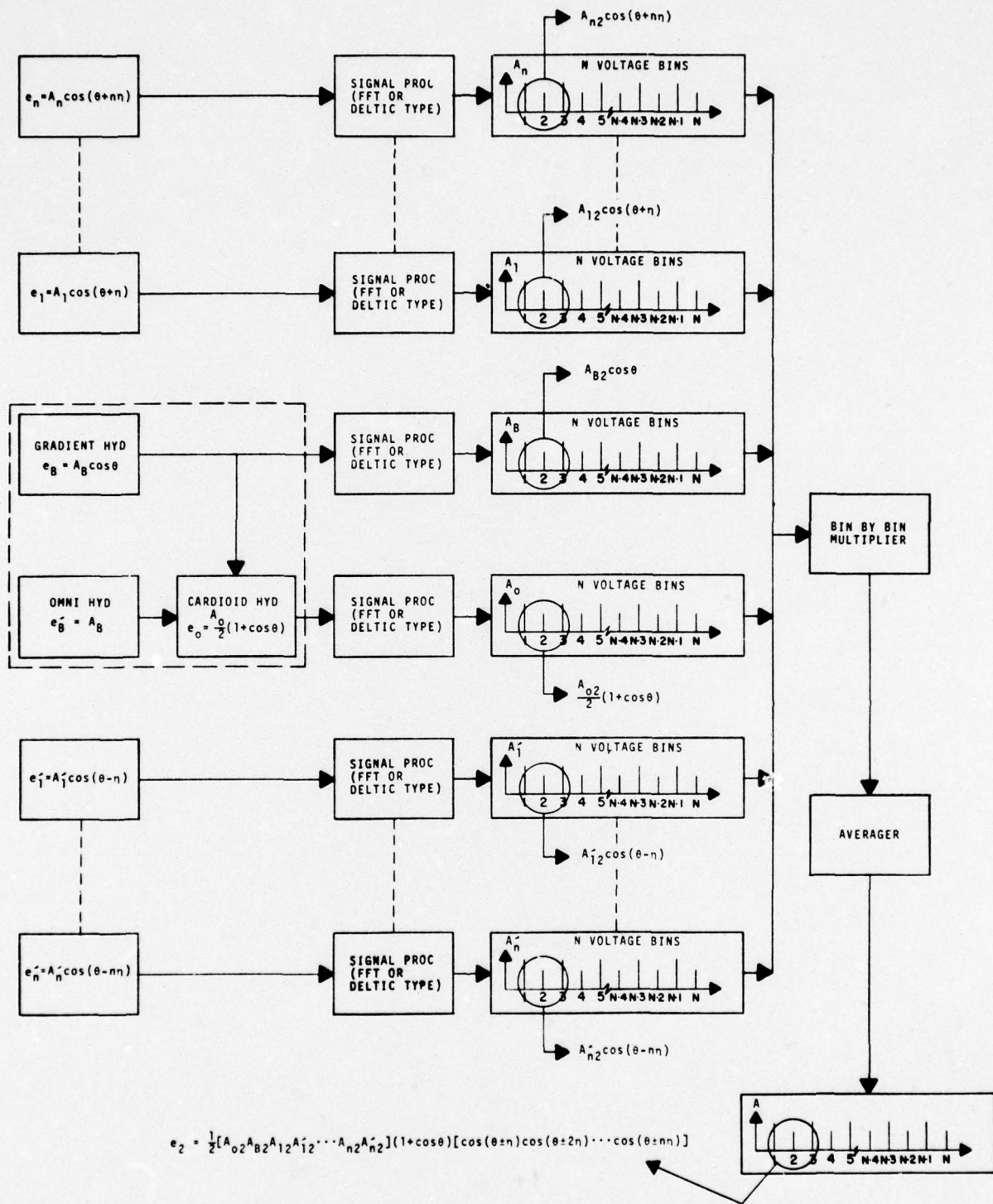
3

$A_{n2}\cos(\theta+n\eta)$

$e_n = A_n\cos(\theta+n\eta)$

SIGNAL PROC (FFT OR DELTIC TYPE)

A_n N VOLTAGE BINS

1 2 3 4 5 N-4 N-3 N-2 N-1 N

$A_{12}\cos(\theta+\eta)$

$e_1 = A_1\cos(\theta+\eta)$

SIGNAL PROC (FFT OR DELTIC TYPE)

A_1 N VOLTAGE BINS

1 2 3 4 5 N-4 N-3 N-2 N-1 N

$A_{B2}\cos\theta$

GRADIENT HYD $e_B = A_B\cos\theta$

SIGNAL PROC (FFT OR DELTIC TYPE)

A_B N VOLTAGE BINS

1 2 3 4 5 N-4 N-3 N-2 N-1 N

OMNI HYD $e'_B = A_B$

CARDIOID HYD $e_0 = \frac{A_0}{2}(1+\cos\theta)$

SIGNAL PROC (FFT OR DELTIC TYPE)

A_0 N VOLTAGE BINS

1 2 3 4 5 N-4 N-3 N-2 N-1 N

$\frac{A_{02}}{2}(1+\cos\theta)$

BIN BY BIN MULTIPLIER

$e'_1 = A'_1\cos(\theta-\eta)$

SIGNAL PROC (FFT OR DELTIC TYPE)

A'_1 N VOLTAGE BINS

1 2 3 4 5 N-4 N-3 N-2 N-1 N

$A'_{12}\cos(\theta-\eta)$

AVERAGER

$e'_n = A'_n\cos(\theta-n\eta)$

SIGNAL PROC (FFT OR DELTIC TYPE)

A'_n N VOLTAGE BINS

1 2 3 4 5 N-4 N-3 N-2 N-1 N

$A'_{n2}\cos(\theta-n\eta)$

$e_2 = \frac{1}{2}[A_{02}A_{B2}A_{12}A'_{12}\cdots A_{n2}A'_{n2}](1+\cos\theta)[\cos(\theta\pm\eta)\cos(\theta\pm2\eta)\cdots\cos(\theta\pm n\eta)]$

A N VOLTAGE BINS

1 2 3 4 5 N-4 N-3 N-2 N-1 N

Figure 2.   "N" Section Array Signal Processing Block Diagram

4

The CTASS method of beamforming is illustrated in figure 3. For example, consider a two-section array and a canted angle. The two-section array
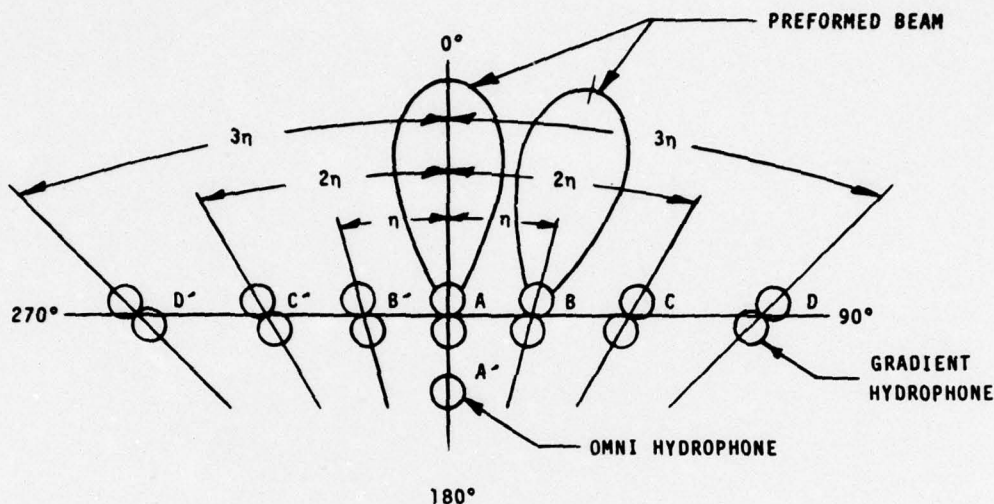

Figure 3. CTASS Beam Forming Example

would use five hydrophones (four gradient and one omni) to beamform. To form a beam in the 0° direction, the basic processing unit (BPU) would be formed with A and A' hydrophones and augmented with the outputs of hydrophones B, B', C, and C'. A beam could be formed in the 180° direction by using the same hydrophones and reversing the polarity of the output from the A hydrophone. Reversing the polarity of the BPU's gradient hydrohone would shift the major response axis from 0° to 180°.

A beam may be formed in the η° direction by using the hydrophone whose main response axis is in the η° direction, to form the BPU; i.e., the BPU would consist of hydrophones B and A'. A two-section array would now be obtained by augmenting the BPU with hydrophones C, A, D, and B'. A beam could be formed in the ($\eta = 180^\circ$) direction by using the same hydrophones, but reversing the polarity of hydrophone B.

5

The net effect of CTASS beamforming is a pattern that would be invariant with respect to the steered direction, and therefore should result in an array gain that would be constant with respect to the steered direction.

The single target beam response of this array showed that apparently quite narrow response patterns could be achieved while having no requirement on element spacing (except in angle). CTASS thus appeared to offer something akin to super gain. Figure 4 shows the comparative single target characteristics for arrays consisting of up to six hydrophone sections.

The signal processing properties of the CTASS system were analyzed under several operational conditions (reference 1). As far as possible, general expressions were developed for the output mean, variance, and signal-to-noise ratio at the output of the averager. In addition, a method was described by which false-alarm probabilities could be evaluated under certain conditions. Because of the exceedingly complex nature of the mathematical expressions involved (theoretical analysis of multiplicative processing is very difficult, and the difficulty increases rapidly with the
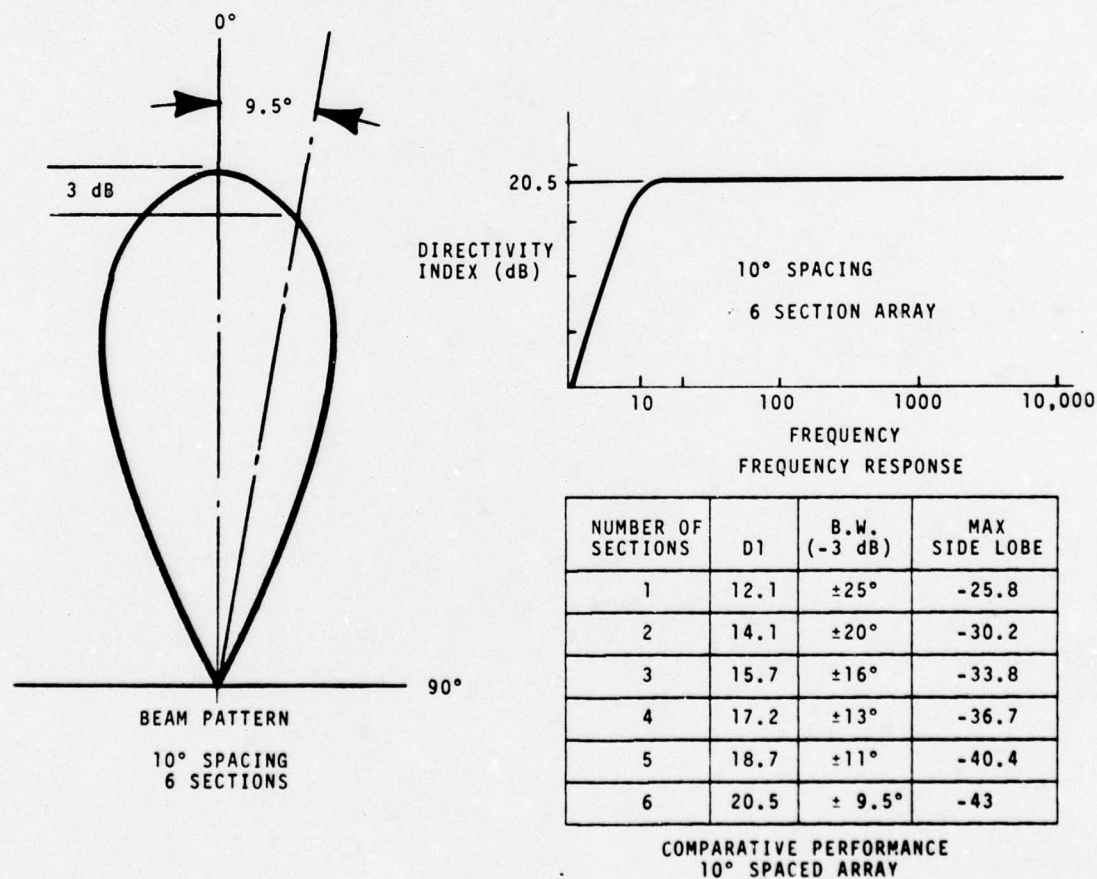

BEAM PATTERN
10° SPACING
6 SECTIONS

FREQUENCY RESPONSE

NUMBER OF SECTIONS	DI	B.W. (-3 dB)	MAX SIDE LOBE
1	12.1	±25°	-25.8
2	14.1	±20°	-30.2
3	15.7	±16°	-33.8
4	17.2	±13°	-36.7
5	18.7	±11°	-40.4
6	20.5	± 9.5°	-43

COMPARATIVE PERFORMANCE
10° SPACED ARRAY

Figure 4. CTASS Array Characterisicts as Affected by Number of Sections

6

number of multiplications), numerical values for the output variance and output signal-to-noise ratio were obtained only for a CTASS array containing two and four elements. The results of this analysis showed that the output signal-to-noise ratio of the CTASS processor would be superior to a conventional linear processor using the same number of sensors. In addition, the CTASS resolution was investigated by analyzing array output for various operational conditions when two targets are present. This analysis indicated poor resolving capabilities when targets were identical (both in power level and frequency content) and separated less than 90°. However, this analysis was made on a broadband basis, and it was felt that a narrowband processing system (as proposed for the operational system) would provide the expected good performance.

The Applied Physics Laboratory (APL) of Johns Hopkins University (reference 2), has made a limited evaluation of CTASS, using simulated isotropic noise and discrete samples of target signals. APL's simulation results showed the same discouraging trend of decreasing detection probability with increasing CTASS array size. However, Electric Boat had serious doubts about the validity of the APL simulation model and the method of performance evaluation, so the task reported here was proposed.

To resolve these issues, it was proposed that a suitable test be evolved to establish the concept's feasibility in the static mode. Since the difficulty of analysis arises from the mathematical complexities of the noise terms, it was suggested that an experimental investigation be undertaken in which real background noise data would be employed. Since it is anticipated that the CTASS would be ambient noise limited, the required background noise would consist only of sea state noise. The recorded noise data would then be used in a computer simulation that would parametrically evaluate the CTASS's usability for antisubmarine warfare. This report describes that investigation and includes descriptions of the test program, the simulation model, and the results.

OBJECTIVE

The objective of this project was to demonstrate the feasibility of the CTASS concept as an alternative to conventional towed sonar arrays. To that end, a two-stage static mode test was undertaken. In the first stage, a horizontal CTASS array was used to acquire real background noise at the Exhuma Sound Acoustic Range. During the second stage, data re-

cordings of individual hydrophone receptions were used to evaluate the
CTASS array's ability to detect targets through computer simulations
carried out at Electric Boat Division's Data Reduction Center. Beam
patterns, beam forming capabilities, and array sensitivities, as affected
by array sections (i.e., number of hydrophones), were to be evaluated
and compared with those obtained from a linear array of an equal number
of omnielements when narrowband target(s) signals are present.

TEST PROGRAM

Test Array

The array configuration as tested appears in figure 5. This array consis-
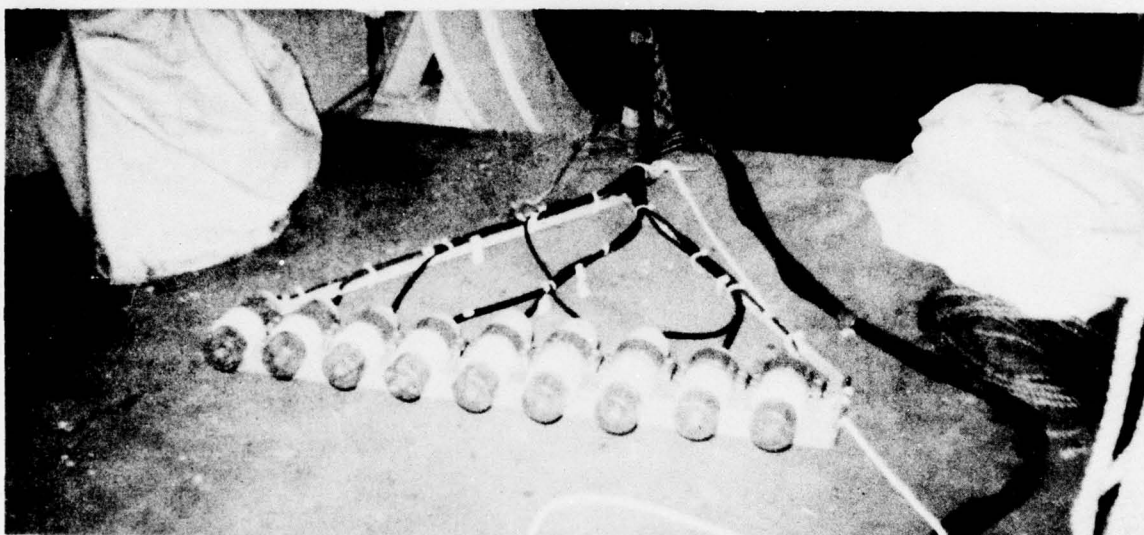ted of nine gradient and six omnidirectional hydrophones. These hydrophones

Figure 5. CTASS Static Test Array

were components of hydrophone assemblies from dismantled DIFAR buoys.
The orientation of the hydrophones within the array is highlighted in
figure 6, which indicates that the angle used is 10°, and that the
hydrophone elements are mounted at 6-in. intervals. The array has an ap-
propriate number of hydrophones to evaluate its performance, with as many
as four hydrophone sections for a broadside beam (nine gradient and one
omnihydrophones), three hydrophone sections for a beam at $\pm 10^O$ (seven
gradient and one omnihydrophones), and two sections for a beam at $\pm 20^O$
(five gradient and one omnihydrophone). All hydrophones were calibrated
for sensitivity in the 100 to 2400 Hz band. In addition, beam patterns

8

were measured for all of the gradient hydrophones at 150, 300, and 2000 Hz. Figure 7 is a typical calibration beam pattern for a gradient hydrophone. Typical sensitivities, at the indicated frequencies for each of the hydrophones, appear in figure 6. Each hydrophone assembly, prior to calibration, was pressure tested to a pressure equivalent to a 200-ft submergence.
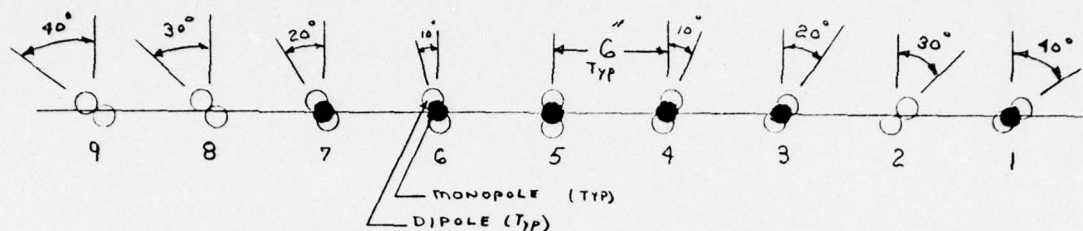
Phone No.	Description	Cal. Sensitivity db v/l microbar	
1	Dipole	-92	
2		-93	
3		-93	
4		-90	
5		-85	Avg. 300 to 1000 Hz
6		-85	
7		-85	
8		-90	
9	Dipole	-91	
1	Monopole	-92	
3		-93	
4		-94	
5		-93	Avg. 500 to 600 Hz
6		-93	
7	Monopole	-93	

Figure 6. CTASS Test Array Hydrophone Orientation and Sensitivity

Data Acquisition

The CTASS static test array was used to measure ambient sea noise at the Exhuma Sound Acoustic Range during the week beginning 28 March 1976. The array was suspended 100 ft below the sea surface, and hydrophone outputs were recorded on magnetic tape. While the prime purpose of this experiment was to measure ambient noise only, several "cuts" were made with a target submarine in the test range vicinity. A total of eleven 5-minute test events were recorded when no traffic was present; two events were recorded with a submarine on the surface 6000 yd from the test sight, and five events were recorded when the submarine was making a submerged run through the test area. For the present effort, however, analysis was performed only on the ambient sea noise data.

Data was acquired by analog recording all unprocessed hydrophone outputs on a 14-channel tape recorder with time code and voice notation. Referring to the equipment depicted in figure 8, a tape recording speed of 30 ips yielded about 15 minutes of test data per reel, with the 20 dB pads providing the signal reduction necessary for tape recorder compatibility.
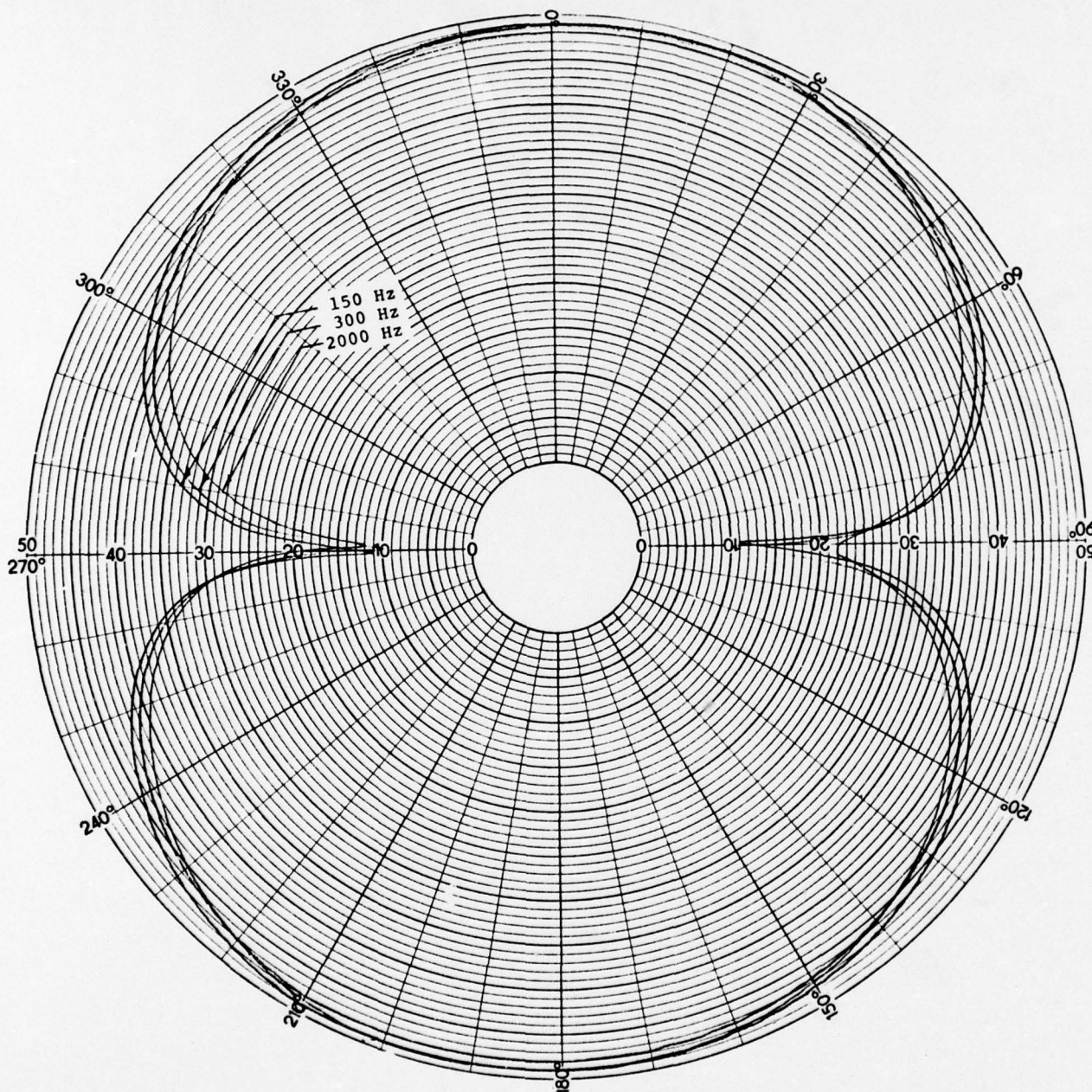

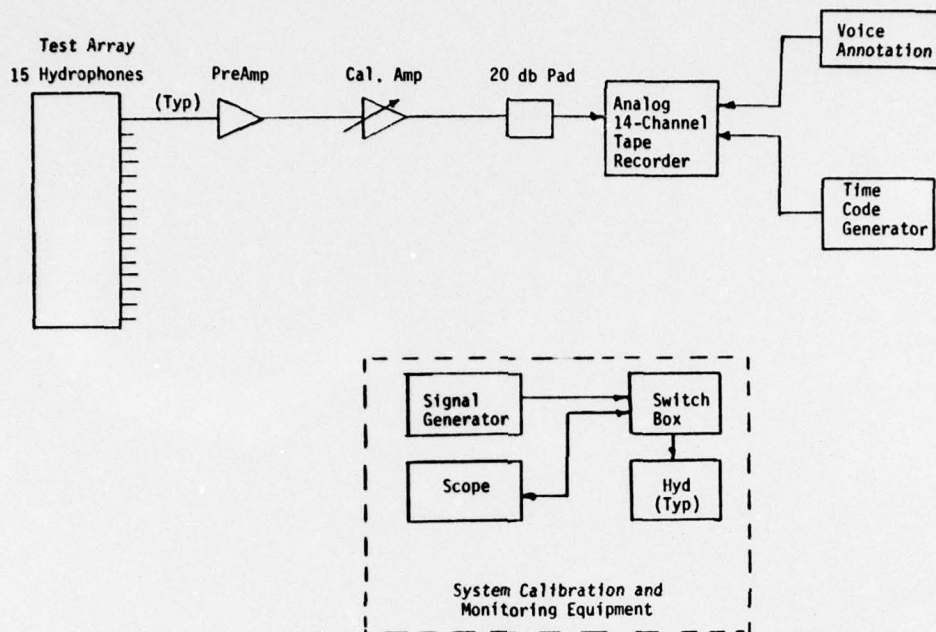Figure 7. Gradient Hydrophone Calibration Beam Pattern

10

Figure 8.   Data Acquisition Equipment Setup

To ensure that a proper reference to input sound pressure level was obtained, the system was calibrated and tape recorded at 1/3 octave center frequencies.   A minimum frequency range of 150 Hz to 3 kHz was recorded.

Since there was a possibility of recording radiated noise from targets of opportunity along with the background noise, the data were verified and edited.   As shown in figure 9, data recordings of an omnihydrophone were
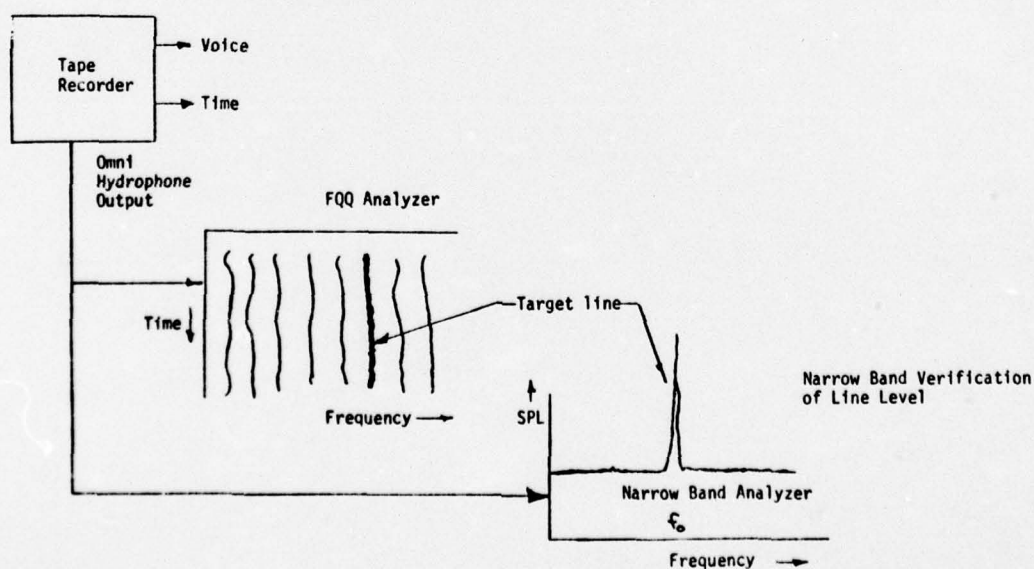

Figure 9.   Data Editing

11

processed through an FQQ analyzer. The resultant frequency versus time presentation, coupled with the time code information, was used to evaluate which events truly depict background noise or a target of opportunity. To verify that the spectral levels were correct, narrowband frequency spectra were produced for selected events.

The noise data were reduced into usable form by first passing them through an analog filter. The analog bandpass filters were General Radio frequency-selective 8% filters (3 dB bandwidth is 8% of selected center frequency). For convenience, a tap was made of the bandpass-filtered noise waveform. These noise data were then converted into a suitable digital format compatible with the storage capabilities of the computer. These stowed noise data were then available for use in the simulation stage of the investigation.

SYSTEM SIMULATION

The raw hydrophone noise information was converted into CTASS array performance evaluation data by simulation. In general, a synthesized signal and interference (after suitable weighting dependent upon the detection operation being simulated , and the hydrophone's directivity response) were operated upon and considered to be that hydrophone's output response as if it were receiving actual target signal(s) and/or interferences, plus the background noise. This combining of in situ noise, plus the synthesized signal(s) would allow for the evaluation of a wide range of signal, noise, array parameters, and geometry. Data processing after that point paralleled that which would occur in an operational system for an individual frequency bin. Figure 10 shows the basic analysis process.

The first step in the processing procedure was to pass the hydrophone output through a narrow band digital filter. The filtered output was then multiplicatively combined with that from companion hydrophones, and averaged to develop the directional character of the array. The output of the averager could then be analyzed to form the desired statistical quantities needed to predict array performance. A detailed description of the signal processing used in the simulation program appears in appendix A.
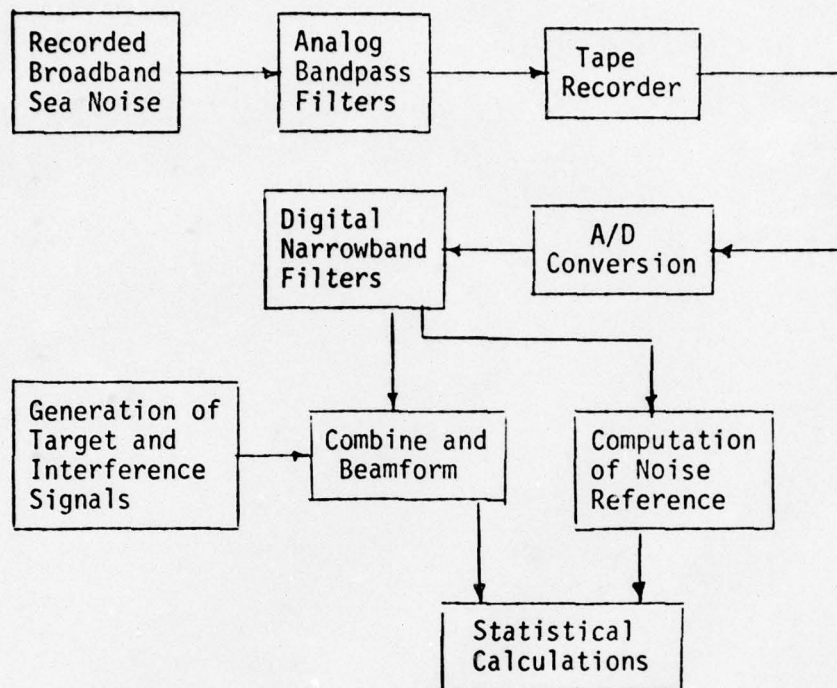
12

Figure 10. Block Diagram of CTASS Analysis Program

13

In each simulation run, the quantity of interest is the output of the integrator $r(T)$ (which depends on integration time T) and its statistics (mean value and variance). Plane-wave propagation is assumed for signal and interference, with direction angles θ_S and θ_I, respectively. Pure sine waves are assumed with peak amplitudes P_S and frequencies f_o and $f_o(1 + \Delta f_o)$, respectively. Initial phase angles are taken to be zero for convenience. We thus have:

$$Z = \underbrace{(y_{oo}y_o')}_{\substack{m = 2 \text{ (BPU)}}} \cdot (y_1 \, y_{-1}) \cdot (y_2 \, y_{-2}) \cdot (\qquad) ---- \tag{1}$$

$$m = 4 \text{ (1 section) etc}$$

$$= Z_m(k\Delta t)$$

and:

$$r_m(T) = \frac{1}{T} \sum_{k=1}^{n} Z_m(k\Delta t) \tag{2}$$

where: $T = n\Delta t$

Δt = A/D conversion sampling time

$y_i(k\Delta t)$ = Noise + Signal at output of digital filter

The statistics are formed by averaging over several T-second intervals. Letting r_i be the output of the integrator for a given array when n_i samples are integrated, we define the mean value as:

$$\bar{r} = \frac{1}{L} \sum_{i=1}^{L} r_i \tag{3}$$

and the mean-squared value as:

$$\bar{r}^2 = \frac{1}{L} \sum_{i=1}^{L} r_i^2 \tag{4}$$

14

The variance is given by:

$$\sigma^2 = \overline{r^2} - (\overline{r})^2 \tag{5}$$

We distinguish between the following three cases:

Noise only present (N).
Signal and noise present (S + N).
Signal plus interference plus noise present (S + I + N).

The output signal-to-noise ratio is defined as:

$$\left(\frac{S}{N}\right)_o = \frac{(\Delta\overline{r})^2}{\sigma^2_{S+N}} \tag{6}$$

where $\Delta\overline{r}$ is the shift in the mean value caused by the presence of the signal:

$$\Delta\overline{r} = \overline{r}_{S+N} - \overline{r}_N$$

Input signal-to-noise ratio is defined as the ratio of signal power, $(P_S^2/2)$, to the noise power that is measured by the omnidirectional hydrophone. An appropriate scaling factor must be included to account for the effects of the hydrophone sensitivity, tape recorder, analog filter, A/D conversion and digital filter bandwidth. Input S/N ratio is referred to as $\left(\frac{S}{N}\right)_i$.

It was anticipated that the following four series of tests would be conducted:

1. The <u>beam pattern</u>, defined as $\overline{r}(\theta_s)$, which depends on frequency f_o and on $\left(\frac{S}{N}\right)_i$.

2. <u>Output S/N ratio</u>, defined as

$$\left(\frac{S}{N}\right)_o = \frac{\overline{r}_{S+N} - \overline{r}_N^{\;2}}{\sigma^2_{S+N}} \tag{7}$$

where σ^2_{S+N} is the variance produced by signal plus noise, as given by equation (5).

15

3. The _interference effect_, evaluated first with respect to the change in mean value caused by the introduction of an interference; i.e., we will calculate:

$$\Delta \bar{r}_I = \bar{r}_{S+I+N} - \bar{r}_{S+N} \tag{8}$$

and, then, with respect to the change in $(S/N)_o$:

$$\Delta \left(\frac{S}{N}\right)_o = \frac{\left(\bar{r}_{S+I+N} - \bar{r}_N\right)^2}{\sigma^2_{S+I+N}} - \frac{\left(\bar{r}_{S+N} - \bar{r}_N\right)^2}{\sigma^2_{S+N}} \tag{9}$$

4. _Resolution_ was to be made for the special case of equal signal and interference amplitude, $P_S = P_I$. For a given run, the angular separation between interference and target remains fixed ($\Delta\theta = \theta_S - \theta_I = $ constant), but the output is evaluated for several values of θ_S. This is equivalent to rotating the array, or to a preformed beam system in which multiple beam outputs are compared. We will evaluate $\Delta\bar{r}$ and $\left(\frac{S}{N}\right)_o$ as a function of θ_S, where

$$\Delta\bar{r} = \bar{r}_{S+I+N} - \bar{r}_N = \Delta\bar{r}_{S+I} \tag{10}$$

and

$$\left(\frac{S}{N}\right)_o = \frac{(\Delta\bar{r}_{S+I})^2}{\sigma^2_{S+I+N}} \tag{11}$$

Table 1 is a compilation of the input and output parameters that were to be varied in the tests. For each test, the variation of the output parameter, as affected by the number of hydrophone sections processed, was to be ascertained for a fixed set of input parameters.

16

Table 1. Test Summary (Anticipated)

Type of Test	Output Parameters	Input Parameters
Beam Patterns	$\overline{r}\,(\theta)$	2 frequencies 2 inputs (S/N) θ_S from 0° to 180°
Output $(S/N)_O$	$\dfrac{(\Delta\overline{r})^2}{\sigma^2_{S+N}} = \left(\dfrac{S}{N}\right)_O$	2 frequencies Several inputs (S/N) $\theta_S = 0^{\circ}$ 2 integration times
Interference effects	$\Delta\overline{r}$ $\left(\dfrac{S}{N}\right)_O$	1 frequency 1 input (S/N) $\theta_S = 0^{\circ}$ Several (I/S) Several θ_I Several Δf_O
Resolution	$\Delta\overline{r}$ $\left(\dfrac{S}{N}\right)_O$	1 frequency 1 input (S/N), $\dfrac{I}{S}$ 2 Δf_O Several $\Delta\theta$ Several θ_S

17

SIMULATION RESULTS

A number of CTASS simulation runs were made using recorded sea noise that had been passed through 8% General Radio analog filters and converted from analog to digital format, as described in appendix A. Frequencies of 525 Hz and 615 Hz were selected. These frequencies were chosen after examining the spectral plots of recorded data. It is believed that essentially only isotropic sea noise was present in the excerpts taken from the tape recorder.

Although the simulation program was developed to handle multiple targets in order to evaluate the resolution and interference discrimination capabilities of CTASS, the first order of business was planned to be a realistic evaluation of the output signal-to-noise ratio $(S/N)_o$. If CTASS did not show promise on the basis of that criterion, no further simulation work was to be performed. The object of the first set of runs was to evaluate the $(S/N)_o$ for the CTASS array consisting of various sections, for "on-target" conditions; i.e., for a simulated target lying on the acoustic axis or main-response axis (MRA). Several values of input signal-to-noise ratios $(S/N)_i$ were used.

The results were very discouraging. Contrary to what had been hoped, it was found that $(S/N)_o$ <u>decreases</u> as the size of the CTASS array increases. In other words, for a given set of fixed inputs to the simulation program (such as sampling frequency, signal amplitude, etc), the output S/N ratio is largest for M = 2 (basic processing unit), then decreases successively for M = 4, 6, 8, and 10. This was found to be the case fairly consistently for several values of $(S/N)_i$.

Earlier analytical work done with broadband signal and noise inputs suggested that this decrease in $(S/N)_o$ might be encountered with increasing number of array elements [1]. The mathematical complexities did not permit a complete analysis of the general CTASS array. Only the basic processing unit (BPU, M = 2) was analyzed fully. A comparison of the output S/N ratio between M = 2 and M = 4 was made in reference (1), but a different definition was used for output S/N ratio. The variance in the

denominator of the S/N ratio equation was taken as being caused by noise only, and the fluctuations caused by the signal were disregarded. This was done for two reasons: to make the analysis more tractable, and because the case of interest in broadband applications is that of small input S/N ratios. For very low values of $(S/N)_i$, the variance with signal present is practically the same as the variance from noise alone. The output S/N ratio thus defined was found to be equal to $28.8 \ (S/N)_i^2 \ B_f T$ for M = 2, and $(23.7(S/N)_i^2 + 96 \ (S/N)^3 + 97 \ (S/N)^4) \ B_f T$ for M = 4. where B_f is the filter bandwidth and T the integration time of the averager. The fact that the $(S/N)_i^2$ coefficient for M = 4 is slightly smaller than the corresponding coefficient for M = 2 gave rise to the suspicion that output SNR might decrease as M increases, but it was thought that the other terms present in the M = 4 expression (which would also be present for higher order systems) might cause the output S/N ratio to increase as M increases, particularly for larger input S/N values (as are present in narrowband applications).

For this reason, it was proposed for the simulation program to evaluate the output S/N first (which now has to include the signal fluctuations because of the larger input signal-to-noise ratios used with narrowband signals) to see whether it increases with M, before any other aspects of CTASS performance were to be evaluated. Further work was to cease if the early results turned out to be disappointing.

Figure 11 shows the ratio of output S/N ratios relative to the basic pro-cessing unit; i.e., we plot R vs M, where:

$$R = \frac{(S/N)_o \ (M \ elements)}{(S/N)_o \ (M = 2)}$$

The input S/N ratios and the number of samples (k) used in the smoothing algorithm are indicated by the arrows in the figure for each curve. It can be seen that R > 1 for M = 4 in two cases. This is probably because of the finite averaging time. Except for these aberrations, the curves are seen to exhibit the same trend, decreasing with increasing values of M. The slope is particularly steep for small $(S/N)_i$ values. However, even for the extremely large values ($(S/N)_i = 2 \times 10^6$ and $K = 10^4$), R is seen to decrease with M.

1.5

✱ THEORETICAL NOISE FREE

$R = \dfrac{(S/N)_0 \ (M \ ELEMENTS)}{(S/N)_0 \ (2 \ ELEMENTS)}$

1.0

0.1

	$(S/N)_i$	NO. OF SAMPLES USED IN INTEGRATION
■	1.1×10^4	100
▢	1×10^6	200
▲	1×10^2	200
△	2×10^6	10,000
◐	1.1	1,000
●	1.0	200

0.01

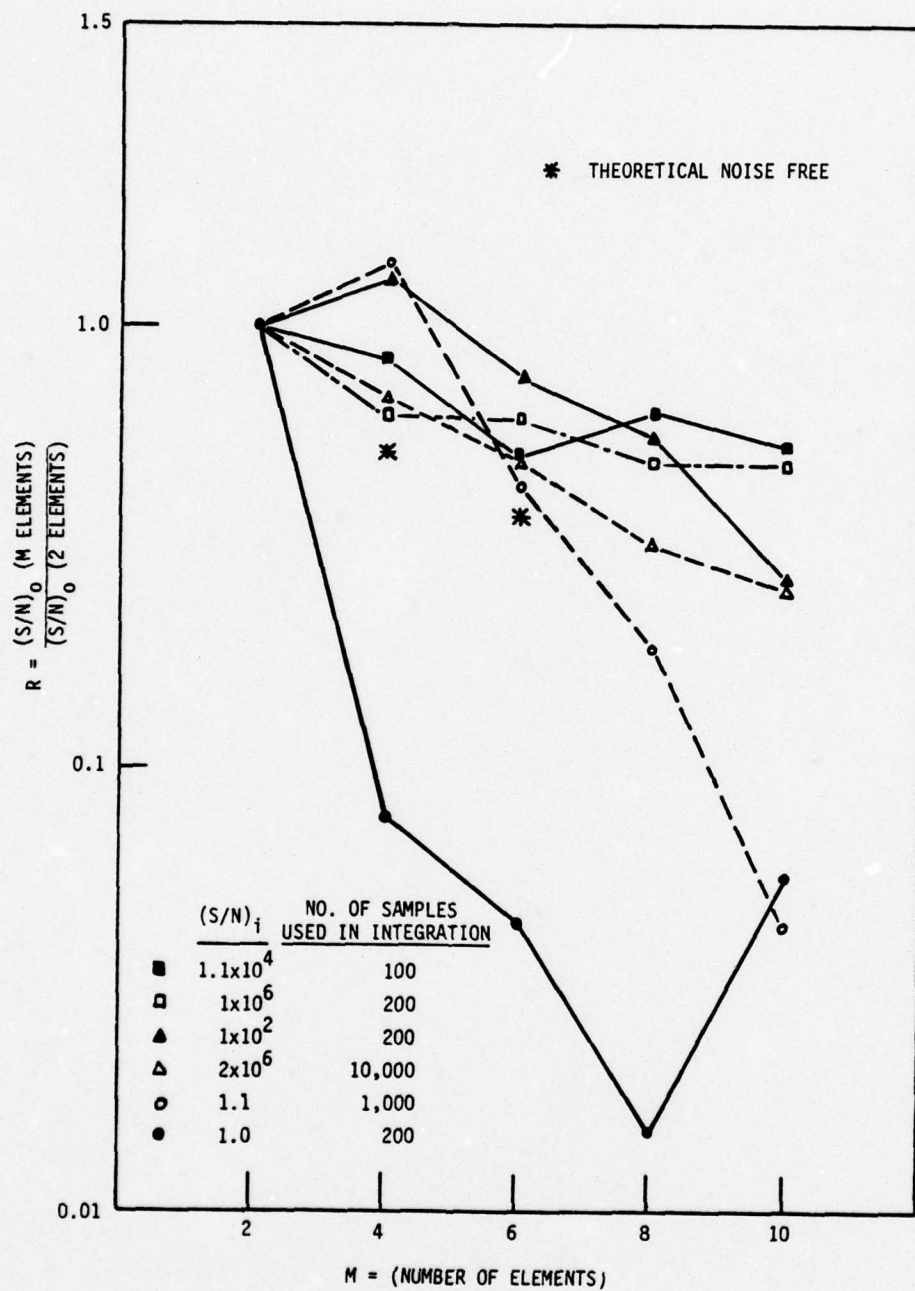2   4   6   8   10

M = (NUMBER OF ELEMENTS)

Figure 11.   Ratio of Output SNR for M Phones
to Output SNR for M = 2

20

The above results prompted us to investigate analytically how $(S/N)_o$ behaves in the noise-free case (output fluctuations because of signal alone). First, we consider the basic processing unit ($M = 2$). Let the target transmit a pure sine wave with peak amplitude P and frequency $f = \omega/2\pi$, and let it be on the MRA (main response axis). The output of the multiplier and integrator is then given by:

$$r(t) = \frac{1}{T} \int_{t-T}^{t} P^2 \cos^2 \omega\tau d\tau$$

$$= \frac{1}{\omega T} \int_{\omega(t-T)}^{\omega t} P^2 \cos^2 x dx$$

$$= \frac{P^2}{2\omega T} \left[x + \frac{1}{2} \sin 2x \right]_{\omega(t-T)}^{\omega\tau} \tag{1}$$

This can be written as:

$$r(t) = \frac{P^2}{2} \left[1 + \frac{a_2 \sin 2\omega t + b_2 \cos 2\omega t)}{2\omega T} \right] \tag{2}$$

where: $a_2 = 1 - \cos 2\omega T$ and

$b_2 = \sin 2\omega T$

We have:

$$r^2(t) = \left(\frac{P^2}{2} \right)^2 \left[1 + \frac{a_2 \sin 2\omega t + b_2 \cos 2\omega t}{\omega T} + \right.$$

$$\left. \frac{a_2^2 \sin^2 2\omega t + b_2^2 \cos^2 2\omega t}{4\omega^2 T^2} + \frac{a_2 b_2 \sin 2\omega t \cos 2\omega t}{2\omega^2 T^2} \right] \tag{3}$$

Output S/N ratio is defined as:

$$\left(\frac{S}{N} \right)_o = \frac{(\bar{r}_{S+N} - \bar{r}_N)^2}{\sigma_{S+N}^2} \tag{4}$$

21

In the noise-free case, this becomes merely:

$$\left(\frac{S}{N}\right)_o = \frac{(\bar{r})}{\overline{r^2} - (\bar{r})^2} \tag{5}$$

where $\bar{r}$ and $\overline{r^2}$ are the average values of equations (2) and (3), respectively. Since the periodic components do not contribute anything to the mean values, we obtain:

$$\bar{r} = P^2/2 \tag{6}$$

$$\overline{r^2} = \left(\frac{P^2}{2}\right)^2 \left(1 + \frac{a_2^2 + b_2^2}{8\omega^2 T^2}\right) \tag{7}$$

But $a_2^2 + b_2^2 = 2(1 - \cos 2\omega T)$. Substituting into equation (5), we get:

$$\left(\frac{S}{N}\right)_o = \frac{4\omega^2 T}{1 - \cos 2\omega T} \tag{8}$$

Note that $(S/N)_o \rightarrow \infty$ as $\cos 2\omega T \rightarrow 1$. This happens when T is very close to an integral number of periods of the signal.

Because of round-off errors, it is not possible in a digital system to make T (which equals $K\Delta t$) exactly equal to an integral number of periods of the frequency before multiplication. Hence, there will be some fluctuations in the output value caused by the signal, and $(S/N)_o$ will be finite even in the noise-free case. In practical applications this is even more true, since the frequency is never known exactly, and since any tone will have a certain amount of modulation.

If we write T as:

$$T = nT_o + \Delta \qquad (n = 1, 2, \ldots) \tag{9}$$

Where $T_o = \frac{1}{f_o} = \frac{2\pi}{\omega}$, we have:

$$2\omega T = 2\omega \left(n \frac{2\pi}{\omega} + \Delta\right) = 4n\pi + 2\omega\Delta \tag{10}$$

$$\cos 2\omega T = \cos(4n\pi + 2\omega\Delta) = \cos 2\omega\Delta \tag{11}$$

For $2\omega\Delta \ll 1$, we can use the approximation:

$$\cos 2\omega\Delta = 1 - \frac{(2\omega\Delta)^2}{2} \tag{12}$$

22

So that:

$$\left(\frac{S}{N}\right)_o \simeq \frac{4\omega^2 T^2}{2\omega^2 \Delta^2} = \frac{2T^2}{\Delta^2} \tag{13}$$

This covers the case M = 2. Equation (8) represents the output S/N ratio for any value of T, and equation (13) is valid for $2\omega\Delta \ll 1$.

To analyze the case M = 4, we proceed in like fashion. We have:

$$r(t) = \frac{1}{T} A_1^2 P^4 \int_{t-T}^{t} \cos^4 \omega\tau \, d\tau \tag{14}$$

where A_1 is the angular sensitivity of the two additional gradient hydrophones (tilted at $\pm 10^\circ$ in our case, making $A_1 = \cos 10^\circ$) to a target on the MRA. We now obtain:

$$r(t) = \frac{A_1^2 P^4}{\omega T} \left[\frac{3}{8} x + \frac{\sin 2x}{4} + \frac{\sin 4x}{32} \right]_{\omega(t-T)}^{\omega t} \tag{15}$$

Carrying out the calculations as in the previous case, we get:

$$(\bar{r})^2 = \left(\frac{3}{8} A_1^2 P^4 \right)^2 \tag{16}$$

$$\overline{r^2} = \left(\frac{3}{8} A_1^2 P^4 \right)^2 \left[1 + \frac{4}{9\omega^2 T^2} \left(\frac{a_2^2 + b_2^2}{2} + \frac{a_4^2 + b_4^2}{128} \right) \right] \tag{17}$$

where a_2 and b_2 are the same as before, and $a_4 = 1 - \cos 4\omega T$, $b_4 = \sin 4\omega T$. Simplifying (17) and subtracting (16), we obtain:

$$\sigma^2 = \left(\frac{3}{8} A_1^2 P^4 \right)^2 \frac{4}{9\omega^2 T^2} \left(1 - \cos 2\omega T + \frac{1 - \cos 4\omega T}{64} \right) \tag{18}$$

Finally,

$$\left(\frac{S}{N}\right)_o = \frac{\frac{9}{4}\omega^2 T^2}{1 - \cos 2\omega T + \frac{1 - \cos 4\omega t}{64}} \tag{19}$$

23

Again, we see that $(S/N)_o \to \infty$ as $\omega T \to n\pi$ $(n = 1, 2, \ldots)$.

Letting $T = nT_o + \Delta$ as before (equation 9), we obtain:

$$\left(\frac{S}{N}\right)_o = \frac{18}{17} \frac{T^2}{\Delta^2} \tag{20}$$

Thus we see that $(S/N)_o$ has decreased when going from $M = 2$ to $M = 4$. Carrying one step further, we analyze the 6-element array $(M = 6)$. Now we get for the output of the integrator:

$$r(t) = \frac{A_1^2 A_2^2 P^6}{T} \int_{\omega(t-T)}^{\omega t} \cos^6 x \; dx \tag{21}$$

Carrying out the mathematical details, we obtain:

$$\bar{r} = \frac{10}{32} A_1^2 A_2^2 P^6 \tag{22}$$

$$\overline{r^2} = \left(\frac{10}{32} A_1^2 A_2^2 P^6\right)^2 \left[1 + \frac{1}{\omega^2 T^2} \left\{\left(\frac{15}{2}\right)^2 (1 - \cos 2\omega T) + \left(\frac{3}{2}\right)^2 (1 - \cos 4\omega T) + \frac{1}{36} (1 - \cos 6\omega T)\right\}\right] \tag{23}$$

The output S/N ratio becomes:

$$\left(\frac{S}{N}\right)_o = \frac{\frac{400}{225} \omega^2 T^2}{1 - \cos 2\omega T + \frac{1 - \cos 4\omega T}{25} + \frac{1 - \cos 6\omega T}{(45)^2}} \tag{24}$$

In terms of Δ, we obtain:

$$\left(\frac{S}{N}\right)_o = \frac{100}{131} \frac{T^2}{\Delta^2} \tag{25}$$

24

We see that the output S/N has suffered another decrease when going from M = 4 to M = 6. If we divide the output S/N ratio obtained for M = 4 and M = 6 by that for M = 2, we obtain for the ratio R = 0.53 for M = 4 and R = 0.38 for M = 6. These values are indicated in figure 11 as asterisks to show the comparison with experimental values.

There is no reason to suppose that this trend of decreasing output S/N ratio with increasing array size would be reversed for M > 6.

CONCLUSIONS AND RECOMMENDATIONS

The agreement between the theoretical and experimental results shown here, coupled with the analysis performed on broadband signals (reference 1) which implied a decreasing output S/N ratio as M increases, leads us to conclude that CTASS in its presently conceived form is not a promising array processing system.

It is entirely possible, however, that some other way of combining the outputs of the gradient hydrophones (e.g., pair-wise multiplication followed by addition and/or split-beam processing), might lead to improved output performance while retaining some of the other CTASS advantages (high maneuverability, directionality, etc). The S/N ratio evaluation of alternate CTASS configurations should be made by analytical methods (as done here for the noise-free case) to the fullest possible extent. If one or more such configurations appear promising, a simulation model comparable with the one used here should be developed. The recorded at-sea data collected during this project could be used. The cost of such an investigation would be modest indeed, since a substantial portion of the necessary groundwork has already been laid.

REFERENCES

1. Izzo, A. J. and Ueberschaer, M. H., "Controlled Towed Array Sur-
    veillance System (CTASS) System Description and Signal Processing
    Analysis (U)," Electric Boat report P440-74-039, April 1974,
    CONFIDENTIAL.

2. Luke, P. J., "Evaluation of a Multiplicative Device - CTASS,"
    Applied Physics Laboratory, Johns Hopkins University, POR-3104,
    September 1974.

Appendix A

CTASS SIMULATION AND DATA REDUCTION PROGRAM

In order to save on computing and storage requirements, it is desired to select as low a sampling rate as possible (that was one reason for using the analog bandpass filters). It is well known that the sampling process causes changes in the spectrum of the original signal. In particular, "aliases" are introduced; that is, other components appear in the spectrum after sampling that were not present before sampling. The mathematical relationship between the spectrum of the sampled signal $F_s(j\omega)$ and the original signal $F(j\omega)$ is

$$F_s(j\omega) = \sum_{k=-\infty}^{\infty} a_k \, F(j\omega - k\omega_s) \tag{1}$$

where $\omega_s = 2\pi f_s$ (f_s = sampling frequency = $1/\Delta t$), and a_k depends on the type of sampling (for impulse sampling assumed here, a_k = constant).

Figure 1 illustrates the sampled spectrum for a narrow-band signal centered at f_o and a sampling frequency of $f_s = \frac{4}{9} f_o$. The shaded portions correspond to the spectrum of the analog signal (before sampling).
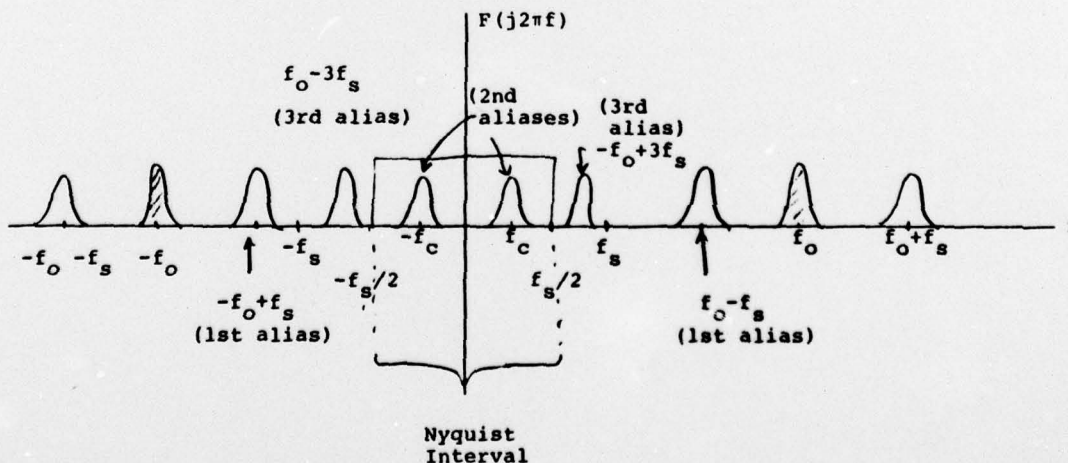

Figure 1. Spectrum of Sampled Signal

A-1

It can be seen that the sampled signal has a rather compli-
cated spectrum. Fortunately, the only portion of the spectrum
which is of direct importance is the part lying inside the
Nyquist interval

$$\frac{-f_s}{2} \leq f \leq \frac{f_s}{2}.$$

For our example, this is the "second alias," namely, the
positive frequency portion shifted by $-2f_s$ and the negative
portion shifted by $+2f_s$.

It can be seen that we have thus effectively "band-
shifted" the data down to a lower frequency by sampling the
data at a rate lower than the frequencies contained in the
original signal. In order to minimize distortion between
aliases, it is desired to have the distance between them as
large as possible. At the same time, we wish to keep our
sampling rate low. The particular choice $f_s = \frac{4}{9} f_o$ is a
good compromise. The interferences caused by the nearest
alias on either side of the spectral component within the
Nyquist interval are made equal (for a symmetrical spectrum,
which is assumed here) by this choice of sampling frequency.

Since the bandwidth B of the analog filters (hence of
the noise spectrum) is .08 f_o, and since the distance between
aliases is $2f_o/9 = 0.2222 \cdots f_o$, the nearest alias is
approximately 5 half-bandwidths away from the spectral com-
ponent of interest. This corresponds to a distortion due to
aliasing of less than 20 db in amplitude, and can be
considered as negligible.

In order to achieve locally high input signal-to-noise
ratios even for low-level signals, it is desired to use
narrowband filters. Because of the difficulty in designing
very narrow bandpass filters, it is more convenient to band-
shift the spectrum down to base-band and use a low-pass
filter to obtain the same end result. This is done by split-
ting the signals up into quadrature components, as will be
shown.

A-2

The target and interference signals need not be filtered, since a sinusoidal signal of known frequency is assumed and is simulated in each case. In an actual system with real signals, the output of the ith hydrophone can be written as

$$v_i(t) = n_i(t) + A_i(\theta)P \cos(\omega_o[t-\tau_i]+\alpha)$$

$$+ A_i(\phi)Q \cos[\omega_o'(t-\sigma_i)+\beta] \qquad (2)$$

where

$\quad\quad n_i(t)$ is the ambient noise

$\quad\quad\quad P$ is the peak amplitude of the target signal

$\quad\quad\quad Q$ is the peak amplitude of the interference signal

$\quad\quad\quad \omega_o$ is the frequency of the target signal

$\quad\quad\quad \omega_o'$ is the frequency of the interference signal

$\quad\quad\quad \theta$ is the target angle relative to the array axis

$\quad\quad\quad \phi$ is the interference angle relative to the array axis

$\quad\quad A_i(\ )$ is the angular beampattern of the ith hydrophone

$\quad\quad\quad \tau_i$ is the geometric delay of the target signal

$\quad\quad\quad \sigma_i$ is the geometric delay of the interference signal

$\quad\quad \alpha, \beta$ are arbitrary phase angles

Since the noise is assumed to be narrowband Gaussian noise, it can be written as

$$n_i(t) = n_{i_c}(t) \cos \omega_o t + n_{i_s}(t) \sin \omega_o t \qquad (3)$$

Without loss of generality, the initial phase angle α can be dropped, and Eq. 2 can be written (using Eq. 3) as

$$v_i(t) = \left(n_{i_c}(t) + P_c + Q_c\right) \cos \omega_o t$$

$$+ \left(n_{i_s}(t) + P_s + Q_s\right) \sin \omega_o t \qquad (4)$$

$$= v_{i_c}(t) \cos \omega_o t + v_{i_s}(t) \sin \omega_o t$$

This is now in the form of the two quadrature components, $v_{i_c}(t) \cos \omega_o t$ and $v_{i_s}(t) \sin \omega_o t$. It can readily be shown that when $v_i(t)$ is multiplied by $2 \cos \omega_o t$ and the output is passed through a low-pass filter, the filtered version of $v_{i_c}(t)$ is obtained. The filtered version of $v_{i_s}(t)$ can similarly be gotten, and the filtered form of $v_i(t)$ can be constructed by multiplying $v_{i_c}(t)$ by $\cos \omega_H t$, $v_{i_s}(t)$ by $\sin \omega_H t$ (ω_H is some convenient frequency, not necessarily equal to ω_o) and adding the two signals.

This procedure will be used in our analysis program, except that the frequency f_c is used instead of f_o, and that the target and interference signals will be simulated as levels P_c, Q_c, P_s, and Q_s, rather than as sinusoidal functions. This simplifies the simulation, but is equivalent. In fact, it also eliminates any phase errors which might result from inaccurate knowledge of the center frequency f_c. The diagram of Fig. 2 illustrates the procedure.

It was drawn for an arbitrary channel. Naturally, for the basic processing unit the outputs of the omniphone and the gradient phase are combined to replace the omni channel. As many as 10 outputs are multiplied at the far right of Fig. 2. Because this gives rise to frequencies up to $10 \omega_H$, care must be taken that the highest frequency is still within the Nyquist band
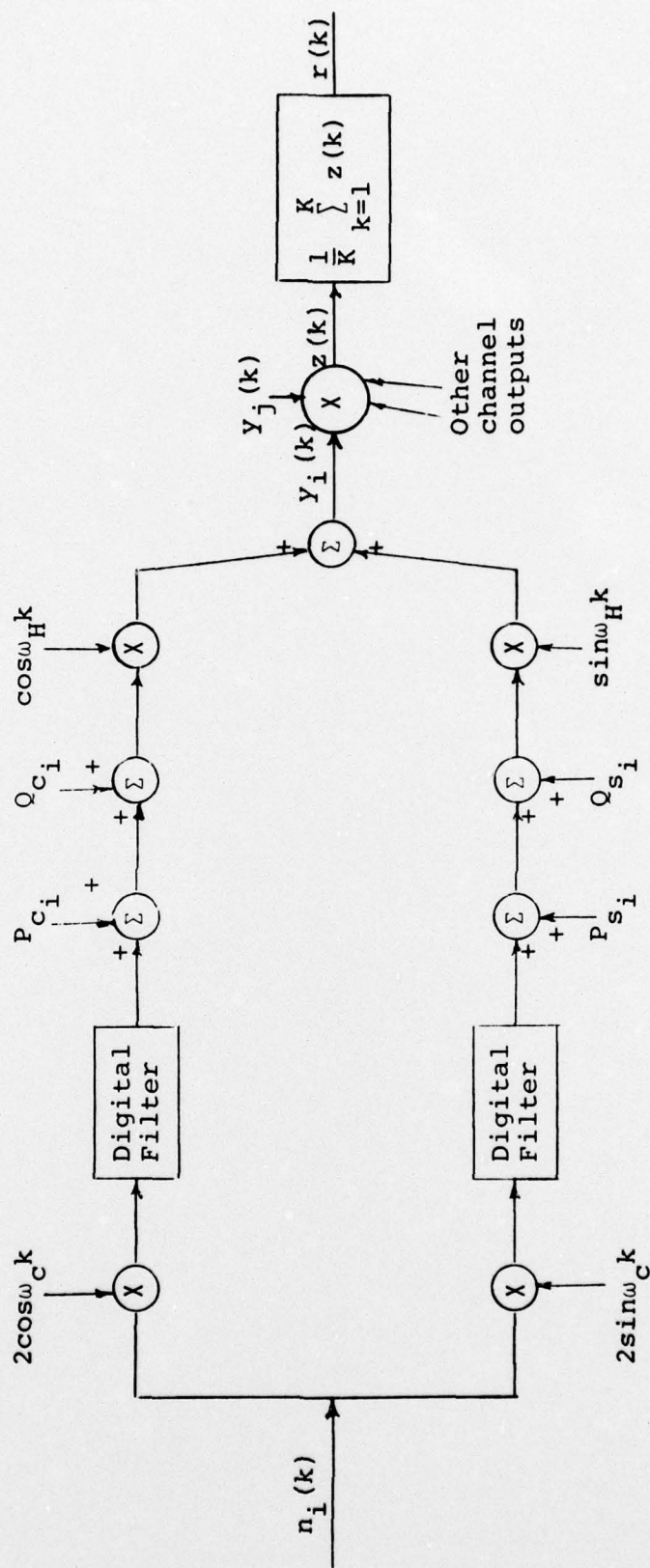
$$-\frac{f_s}{2} \leq f \leq \frac{f_s}{2}$$

FIG. 2. Block Diagram of Digital Analysis Program

A-5

i.e., we require

$$10 \, f_H + \frac{B'}{2} \leq \frac{f_s}{2} \tag{5}$$

where B' is the bandwidth of the digital filter. Since there will also be frequencies of $2f_H$, $4f_H$, $6f_H$, and $8f_H$ present, we also require that there be sufficient separation between them, or that

$$B' < f_H \tag{6}$$

The following limits satisfy these requirements:

$$f_H \leq \frac{f_o}{50} \quad \text{and} \quad B' \leq \frac{f_o}{100}$$

This gives (using the equality),

$$B' = f_H/2 < f_H$$

and, since $f_s = \frac{4}{9} \, f_o$

$$10f_H + \frac{B'}{2} = \frac{f_o}{5} + \frac{f_o}{200} < \frac{4}{9} \, f_o$$

An input frequency of f_o = 500 Hz thus allows us to go up to a bandwidth of B' = 5 Hz.

The notation used is listed below and a complete set of equations for the simulation program is presented. The constants K_i are used to neutralize the effect of different hydrophone sensitivities.

$n'_{oo}(k) = n'_{oo}(k \Delta t)$ = digitized noise from omni phone

$n_{oo}(k)$ = digitized noise from gradient phone with $\eta = 0$

$n_1(k)$ = digitized noise from gradient phone with $\eta = +10°$

$n_{-1}(k)$ = digitized noise from gradient phone with $\eta = -10°$

$n_2(k)$ = digitized noise from gradient phone with $\eta = +20°$

$n_{-2}(k)$ = digitized noise from gradient phone with $\eta = -20°$

$n_3(k)$ = digitized noise rom gradient phone with $\eta = +30°$

$n_{-3}(k)$ = digitized noise from gradient phone.with $\eta = -30°$

$n_4(k)$ = digitized noise from gradient phone with $\eta = +40°$

$n_{-4}(k)$ = digitized noise from gradient phone with $\eta = -40°$

k = $k\Delta t$; $\Delta t = \dfrac{1}{f_s} = \dfrac{9}{4f_o} = \dfrac{2.25}{f_o}$

c = speed of sound

$\tau_i = \dfrac{d_i}{c} \sin\theta$

$\qquad\qquad\qquad i = \pm 1 \text{ to } \pm 4$

$\sigma_i = \dfrac{d_i}{c} \sin\phi$

$a_1 = e^{-\pi B'\Delta t}$, $\quad a_2 = 1 - a$

$n_o(k) = [K'_{oo}n'_{oo}(k) + K_{oo}n_{oo}(k)]$

$n_{o_c}(k) = n_o(k) \cos\omega_c k$

$\left.\begin{array}{l} d_{o_c}(k) = a_1 d_{o_c}(k-1) + a_2 n_{o_c}(k) \\ e_{o_c}(k) = a_1 e_{o_c}(k-1) + a_2 d_{o_c}(k) \end{array}\right\}$ Digital Filter (I)

$x_{o_c}(k) = \ell_{o_c}(k) + \dfrac{P}{2}(1+\cos\theta) + \dfrac{Q}{2}(1+\cos\phi)\cos(\Delta\omega_o k + \beta)$

$y_{o_c}(k) = x_{o_c}(k) \cos\omega_H k$

$$n_{o_s}(k) = n_o(k) \sin \omega_c k$$

$$\left. \begin{array}{l} d_{o_s}(k) = a_1 d_{o_s}(k-1) + a_2 n_{o_s}(k) \\[2mm] \ell_{o_s}(k) = a_1 \ell_{o_s}(k-1) + a_2 d_{o_s}(k) \end{array} \right\} \quad \text{Digital Filter} \quad \text{(I)}$$

$$x_{o_s}(k) = \ell_{o_s}(k) + \frac{Q}{2}(1+\cos\phi)\sin(\Delta\omega_o k + \beta)$$

$$y_{o_s}(k) = x_{o_s}(k) \sin \omega_H k$$

$$y_o(k) = y_{o_c}(k) + y_{o_s}(k)$$

$$n_{oo_c}(k) = 2n(k)_{oo}K_{oo} \cos\omega_c k$$

$$d_{oo_c}, \ell_{oo_c} \text{ as in (I)}$$

$$x_{oo_c}(k) = \ell_{oo_c}(k) + P\cos\theta + Q\cos\phi \cos(\Delta\omega_o k + \beta)$$

$$y_{oo_c}(k) = x_{oo_c}(k) \cos \omega_H k$$

$$y_{oo}(k) = y_{oo_c}(k) + y_{oo_s}(k)$$

$$n_{oo_s}(k) = 2n_{oo}(k)K_{oo} \sin \omega_c k$$

$$d_{oo_s}, \ell_{oo_s} \text{ as in (I)}$$

$$x_{oo_s}(k) = \ell_{oo_s}(k) + Q\cos\phi \sin(\Delta\omega_o k + \beta)$$

$$y_{oo_s}(k) = x_{oo_s}(k) \sin \omega_H k$$

$$n_i(k) \qquad (i = \pm 1, \pm 2, \pm 3, \pm 4)$$

$$n_{i_c}(k) = [K_i n_i(k) \cos \omega_c k] \times 2$$

$$n_{i_s}(k) = [K_i n_i(k) \sin \omega_c k] \times 2$$

$$d_{i_c}(k) \rightarrow \ell_{i_c}(k) \text{ as in (I)}$$

$$d_{i_s}(k) \rightarrow \ell_{i_s}(k) \text{ as in (I)}$$

$$x_{i_c}(k) = \ell_{i_c}(k) + P \cos(\theta - \eta_i) \cos \omega_o \tau_i$$
$$+ Q \cos\phi - \eta_i) \cos(\Delta \omega_o k + \omega_o' \sigma_i)$$

$$x_{i_s}(k) = \ell_{i_s}(k) + P \cos(\theta - \eta_i) \sin \omega_o \tau_i$$
$$+ Q \cos(\phi - \eta_i) \sin(\Delta \omega_o k + \omega_o' \tau_i)$$

$$y_{i_c}(k) = x_{i_c}(k) \cos \omega_H k$$

$$y_{i_s}(k) = x_{i_s}(k) \sin \omega_H k$$

$$y_i(k) = y_{i_c}(k) + y_{i_s}(k)$$

Now form

$$z_o(k) = y_o(k) y_{oo}(k) \qquad \text{(BPU) } M = 2$$

$$z_1(k) = z_o(k) y_1(k) y_{-1}(k) \qquad \text{(M=4) - 1 section}$$

$$z_2(k) = z_1(k) y_2(k) y_{-2}(k) \qquad \text{(M=6) - 2 section}$$

$$z_3(k) = z_2(k) y_3(k) y_{-3}(k) \qquad \text{(M=8) - 3 section}$$

$$z_4(k) = z_3(k) y_4(k) y_{-4}(k) \qquad \text{(M-10) - 4 section}$$

$$r_j(L) = \frac{1}{L} \sum_{k=1}^{L} z_j(k) \qquad \text{print running average}$$
and store for $L = L_n$

If we integrate over two periods of the lowest frequency of interest ($2\omega_h$), we let

$$T = \frac{2}{2f_H} = \frac{1}{f_H}$$

If $f_H = \frac{f_o}{50}$ and $f_o = \frac{4}{9}f_o$, $\Delta t = \frac{1}{f_s} = \frac{9}{4f_o} = \frac{2.25}{f_o}$

$$T = \frac{1}{f_H} = \frac{50}{f_o}, \qquad L_n = \frac{T}{\Delta t} = \frac{50/f_o}{\frac{9}{4}f_o} = \frac{200}{9}$$

Should get very little fluctuation after an average of about 10 to 20 samples.

Noise Reference

$$n'_{oo_c}(k) = 2n'_{oo}(k)K'_{oo}\cos\omega_c k$$

$$\left.\begin{array}{l} d'_{oo_c}(k) = a_1 d'_{oo_c}(k-1) + a_2 n'_{oo}(k) \\[6pt] \ell'_{oo_c}(k) = a_1 \ell'_{oo_c}(k-1) + a_2 d'_{oo_c}(k) \end{array}\right\} \qquad \text{Dig. Filter (I)}$$

$$x'_{oo_c} = \ell'_{oo_c}(k)$$

$$y'_{oo_c}(k) = x'_{oo_c}(k)\cos\omega_H k$$

$$n'_{oo_s}(k) = 2n'_{oo}(k)K'_{oo}\sin\omega_c k$$

$$\left.\begin{array}{l} d'_{oo_s}(k) = a_1 d'_{oo_s}(k-1), \text{ etc.} \\[6pt] \ell'_{oo_c}(k) \quad \ldots \end{array}\right\} \qquad \text{Dig. Filter (I)}$$

$$x'_{oo_s} = \ell'_{oo_c}$$

$$y'_{oo_s}(k) = x'_{oo_s}(k)\sin\omega_H k$$

$$y'_{oo}(k) = y'_{oo_c}(k) + y'_{oo_s}(k) \qquad\qquad N = \frac{1}{K}\sum_{k=0}^{K}[y'_{oo}(k)]^2$$

A-10

The first set of equations with the subscripts o and oo
apply to the basic processing unit. The next set of
equations are for added sections. Because many of the
equations are repeated (only the subscripts differ), only
the general subscript i was used. The digital filter
equation denoted by (I) is repeated again and again and
is thus subsequently merely referenced by (I).

REPORT DOCUMENTATION PAGE		READ INSTRUCTIONS BEFORE COMPLETING FORM
1. REPORT NUMBER CTASS-77-01	2. GOVT ACCESSION NO.	3. RECIPIENT'S CATALOG NUMBER
4. TITLE (and Subtitle) Controlled Towed Array Surveillance System (CTASS) Array Static Test and Simulation.		5. TYPE OF REPORT & PERIOD COVERED Final rept.
		6. PERFORMING ORG. REPORT NUMBER
7. AUTHOR(s) A. J. Izzo M. H. Ueberschaer		8. CONTRACT OR GRANT NUMBER(s) N00039-76-C-0169
9. PERFORMING ORGANIZATION NAME AND ADDRESS GENERAL DYNAMICS Electric Boat Division Groton, Connecticut 06340		10. PROGRAM ELEMENT, PROJECT, TASK AREA & WORK UNIT NUMBERS 41 p.
11. CONTROLLING OFFICE NAME AND ADDRESS Naval Electronic Systems Command Washington, D. C. 20362		12. REPORT DATE January 1977
		13. NUMBER OF PAGES 36
14. MONITORING AGENCY NAME & ADDRESS(if different from Controlling Office) Underwater Surveillance Division (ELEX 3203) Washington, D. C. 20362		15. SECURITY CLASS. (of this report) Unclassified
		15a. DECLASSIFICATION/DOWNGRADING SCHEDULE

16. DISTRIBUTION STATEMENT (of this Report)

DISTRIBUTION STATEMENT A
Approved for public release;
Distribution Unlimited

17. DISTRIBUTION STATEMENT (of the abstract entered in Block 20, if different from Report)

18. SUPPLEMENTARY NOTES

19. KEY WORDS (Continue on reverse side if necessary and identify by block number)

Passive Sonar; Multiplicative Processing; Gradient Elements; Towed Array; Test; Simulation

20. ABSTRACT (Continue on reverse side if necessary and identify by block number)

An evaluation of the Controlled Towed Array Surveillance System (CTASS) was made by using recorded sea noise as received with CTASS sensors, filtering and digitizing the noise data, simulating sinusoidal target signals, and simulating CTASS performance with respect to output ratio, $(S/N)_o$. It was found that $(S/N)_o$ decreases as the array size is increased. This disturbing trend prompted an analytical investigation using noise-free conditions, but assuming realistic integration times. That analysis confirmed

DD FORM 1473 EDITION OF 1 NOV 65 IS OBSOLETE
1 JAN 73
S/N 0102-014-6601
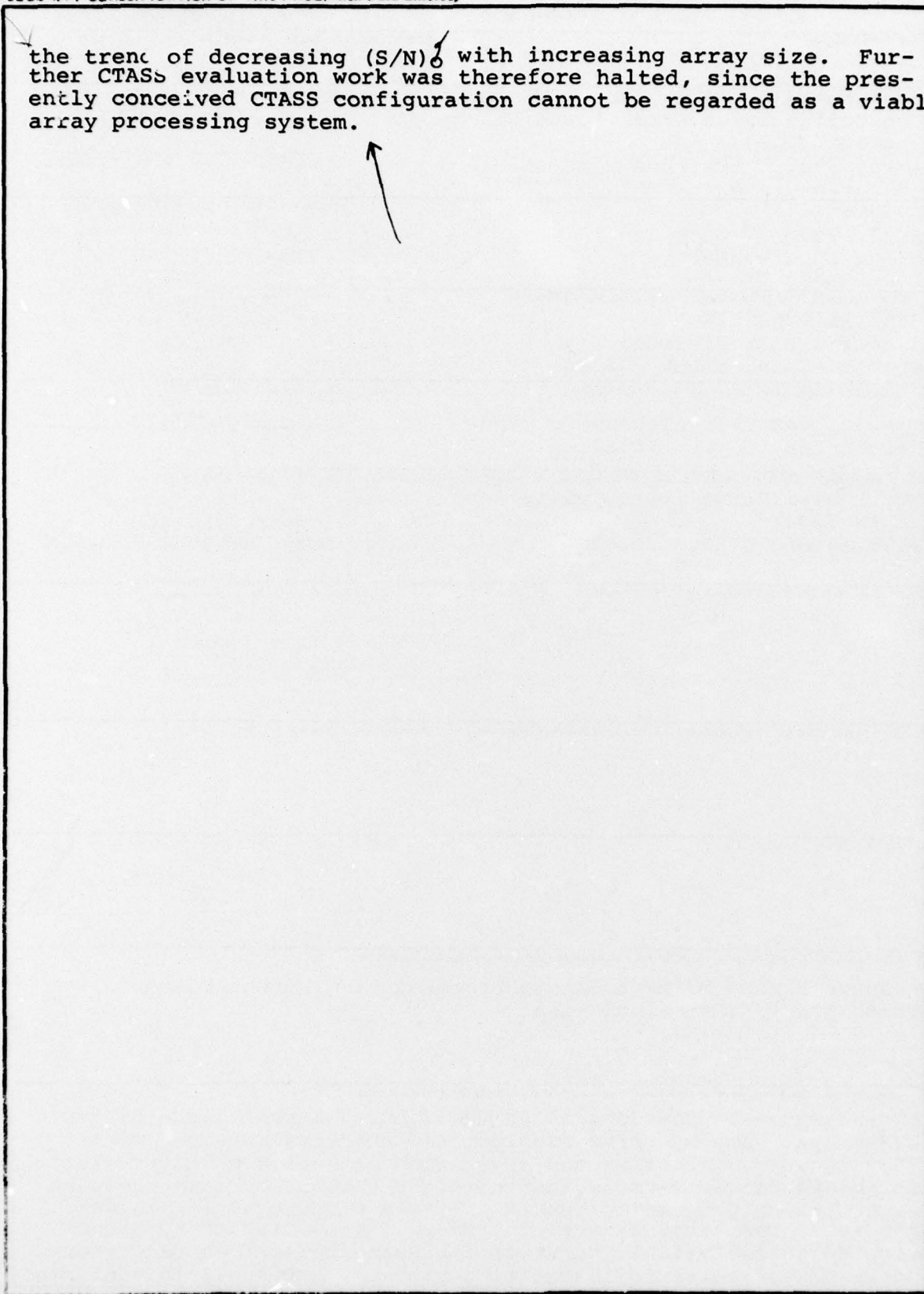
123150

the trend of decreasing $(S/N)_o$ with increasing array size. Further CTASS evaluation work was therefore halted, since the presently conceived CTASS configuration cannot be regarded as a viable array processing system.